Acta Agronómica (2020) 69 (4) p 293-305 ISSN 0120-2812 | e-ISSN 2323-0118 doi: https://doi.org/10.15446/acag.v69n4.89795

UNIVERSIDAD NACIONAL DE COLOMBIA

Dryer design parameters and parts specifications for an industrial scale bagasse drying system

Parámetros de diseño del secador y especificaciones de piezas para un sistema de secado de bagazo a escala industrial

Greg Wheatley [1], Rong Situ [2], Jarrod Dwyer [3], Alexander Larsen [4], Robiul Islam Rubel [5],

[1]Greg Wheatley. James Cook University, Townsville, Australia. Greg.wheatley@jcu.edu.au
[2]Rong Situ. James Cook University, Townsville, Australia. Rong.situ@jcu.edu.au
[3]Jarrod Dwyer. James Cook University, Townsville, Australia. Jarrod.dwyer@my.jcu.edu.au
[4]Alexander Larsen. James Cook University, Townsville, Australia. Alexander.larsen@my.jcu.edu.au
[5]Robiul Islam Rubel. Bangladesh Army University of Science and Technology, Saidpur 5310, Bangladesh. rubel.ruet10@yahoo.com

Rec:06-08-2020 Acep:29-09-2020

Abstract

The sugar industry is an ideal sector for electricity cogeneration due to a large amount of burnable bagasse produce as a by-product. Bagasse produced in the sugar industry always consists of moisture affecting the efficiency of a boiler in the cogeneration plant. In our case study, a cogeneration plant run by bagasse burning found with bagasse moisture problem and suffocating with low power generation for the last few years. The boiler efficiency per tonne of bagasse is currently lower than optimal due to the substantial percentage of water present in the bagasse. A bagasse dryer design for this industry can improve the efficiency of a boiler as well as the cogeneration plant. In this paper, a pneumatic bagasse drying system is proposed to reduce the moisture content of bagasse from 48% to 30%. This work provides a full analysis of bagasse dryer design parameters, including specifications for dryer system components, such as feeders, fan, drying tube, and cyclone. The total bagasse drying system proposed is expected to be fitted within a 6 × 6 × 25 m space to dry 60 tph of bagasse, reducing the moisture content from 48% to 30%, in full compliance with all relevant Australian and company standards.

Keyword: Electricity cogeneration; Industry by-product; Moisture content; Sugar industry

Resumen

La industria azucarera es un sector ideal para la cogeneración eléctrica debido a la gran cantidad de bagazo que se produce como subproducto. El bagazo producido en la industria azucarera siempre consiste en humedad que afecta la eficiencia de una caldera en la planta de cogeneración. En nuestro caso de estudio, una planta de cogeneración operada por la quema de bagazo se encontró con un problema de humedad del bagazo y asfixiada con baja generación de energía durante los últimos años. La eficiencia de la caldera por tonelada de bagazo es actualmente inferior a la óptima debido al porcentaje sustancial de agua presente en el bagazo. Un diseño de secador de bagazo para esta industria puede mejorar la eficiencia de una caldera y de la planta de cogeneración. En este trabajo, se propone un sistema de secado neumático de bagazo para reducir el contenido de humedad del bagazo del 48% al 30%. Este trabajo proporciona un análisis completo de los parámetros de diseño del secador de bagazo, incluidas las especificaciones de los componentes del sistema del secador, como alimentadores, ventiladores, tubos de secado y ciclones. Se espera que el sistema de secado total de bagazo propuesto se instale en un espacio de 6 × 6 × 25 m para secar 60 tph de bagazo, reduciendo el contenido de humedad del 48% al 30%, en total cumplimiento con todas las normas relevantes de Australia y de la empresa.

Palabra clave: Cogeneración de electricidad; Contenido de humedad; Subproducto de la industria; Industria azucarera

Introduction

The sugarcane processing industry produces bagasse as a by-product that persists after the crushing of cane (Raj & Stalin, 2016)(Shrivastav & Hussain, 2013)(Ravichandran, Kavinkumar, Kumar, Prasanth, & Ramkumar, 2017). Around 12% of sugarcane mass becomes bagasse that contains moisture and a small amount of soluble solids (Gilberd & Sheehan, 2013). Bagasse can be a useful waste for co-generation plants such as for power production (To, Seebaluck, & Leach, 2018)(Silva, Schlindwein, Vasconcelos, & Corrêa, 2017). With increasing pressure to find alternative energy generation to that of traditional fossil fuels, an increase in efficiency of the burning of bagasse for energy generation will be beneficial not only for the sugarcane industry but also for society in general (To et al., 2018)(Silva et al., 2017). Moisture is a key factor that affects the efficiency of the burning of bagasse (Abdalla, Hassan, & Mansour, 2018)wherefore, 26 kg/s of bagasse flows with constant rate (proposed design(Shanmukharadhya & Sudhakar, 2007). A proper industrial scale improved design of the bagasse drying system is essential to ensure the resolution of such a problem.

To design a new industrial bagasse drying system, information from a company that can produce 2.16 million tons of crushed cane and produces 63 MW of power from its cogeneration plant was considered. Its bagasse has been used for electricity generation since 2005 and feeds into the Australian power grid for many years. The current operation sees on average 60 tph of bagasse being consumed by a boiler at roughly 48% moisture content. By drying the bagasse (to an average of 30%), the efficiency of the boiler can be increased, resulting in greater profits, and a sustainable system. This paper investigates the designing considerations of an improved bagasse drying system to reduce the moisture content of bagasse fed into the boiler to increase efficiency.

A method of increasing this efficiency is to pre-dry the bagasse. It has been demonstrated that there can be up to an 18% reduction in bagasse use by the boiler with the assistance of pre-drying (Gilberd & Sheehan, 2013). To achieve these aims, an improved bagasse dryer design is needed that will increase the operational efficiency of the boiler, and in turn, produce a higher return on each tonne of cane. The design had to meet the company's requirements. To ensure compliance, the company standard requirements were reviewed to meet all relevant design standards and regulations. Also, the design of a bagasse drying system has been extensively studied from different sources by a team of researchers and the process was well documented and largely parameterized to decide on our design.

Using the required knowledge from the review study, this work studies the design of a bagasse drying system and parts specification that will reduce the amount of moisture in bagasse from approximately 48% to 30% following several subsystem analyses. All the important subsystem components are be studied and identified.

Materials and Methods

The design and performance analysis of the bagasse dryer system was conducted with the standard design compliancy of the Australian company. In the first steps of the work, a risk management study was conducted as specified in AS/NZS ISO 31000:2009 Risk Management - Principles and Guidelines (AS/NZS ISO 31000:2009). The bagasse drying system's installation, operation, and maintenance work requirements were broken down into their logical categories and exposures. The potential risks and related hazards were determined in a brainstorming workshop held by relevant professionals, along with representatives from the company. While completing the risk assessment, factors with potential sustainable development impact were also considered.

Using the "*As low as reasonably possible*" (ALARP) system (Yasseri, 2013) each risk was reviewed and alternate methods or additional controls were identified as per the hierarchy of controls until an effective and practicable level of risk reduction was achieved. To develop the most appropriate drying system for the sugar mill, design requirements were followed to make three major design components as follows-Inlet and outlet feeders to introduce and remove the bagasse from the system,

a. Drying tube to remove moisture from the bagasse,

b. Dry scrubber (cyclone) to separate the dry bagasse from the flue gas.

The proposed bagasse drying system should not physically interfere with the existing plant. The available space for the dryer system was a 6×6 m pad area with a height limit of 25 m. The new dryer was made compatible with the existing plant using the same kind of fittings, pipe diameters etc. Enough care was taken to avoid any accessibility problem of mobile equipment within the existing plant. For simplicity of the design and analysis, the coupling between the flue gas line (boiler exits), and the dryer, the cyclone gas outlet, and the stack is not included in the design. We also excluded the required power supply to the bagasse drying system, and cleaning of the flue gas before being introduced to the dryer is also excluded from the design.

Boiler and bagasse information

The proposed dryer must satisfy the capability of the boiler and bagasse is required to dry before feeding into the boiler. The essential boiler information (Table 1) has been supplied by the company concerning the target boiler. The information regarding bagasse (Table 2) is sourced or provided from the sugar mill.

Dryer design parameters and specifications

Feeder selection

After consultation with the company about the importance of design aspects and design requirements, a weighted decision matrix (Ouye, Facility Technics Facility Management Consulting) was devised for selecting the best-fitted feeder for the dryer design. The rotary feeder has found as the most appropriate choice for both the inlet and outlet feeders (Table 3). Using the boiler and bagasse information (Table 1-2), the required volumetric feed can be calculated as ~0.111 m^3/s.

It should be noted that the bagasse is a relatively light density material and at times due to compaction, flows in a sluggish manner. As such, the fill capacity of the bagasse in the rotor pockets is approximately 60-80%. The worst-case scenario (60%) should be considered to identify the best rotary feeder model that could supply the required feed rate of 0.111 m^3/s. From the available Meyer rotary feeder types (Company Catalogue, Smoot Inc, 2014), a feeder is available to handle bagasse demand of 36 36 inch at 20 RPM (Company Catalogue, Smoot Inc, 2014), capable of transporting 0.113 m^3/s when our design requires 0.111 m^3/s (Table 4).

Considering gear ration of 1:50 between the shaft and the final drive on the motor and 90% efficiency, the required amount of motor power for the selected feeder is 2 hp and the outlet feeder can be specified as the same feeder as the primary feeder (Meyer 36 36 inches rotary feeder (Company Catalogue, Smoot Inc, 2014).

Dryer

Due to the limited space available at the involved sugar mill, the short residence time required to meet the 60 tph throughput (Table 1-2), and the nature of bagasse (fibrous), a flash dryer (or pneumatic dryer) system (Sosa-Arnao & Nebra, 2009)(Borde & Levy, 2006) would be the most appropriate. The hot gas stream, (in this case, flue gas from the boiler) can be used to evaporate the moisture from the bagasse (solid). Following the drying process, separation via a dry scrubber can be implemented. The appropriateness of the type of flash dryer was determined using a weighted decision matrix (Ouye, Facility Technics Facility Management Consulting) (Table 5). and it was determined that the single-pass circular drying tube is the most appropriate for the design that was later approved by engineers from the company with dimensions.

A thin-layer drying model (Vijayaraj, Saravanan, & Renganarayanan, 2007)system COP and water outlets temperatures are investigated. Study shows that both the water mass flow rate and inlet temperature have significant effect on system performances. Test results show that the effect of evaporator water mass flow rate on the system performances and water outlet temperatures is more pronounced (COP increases 0.6 for 1 kg/min was used and it was found that the Page model (Eq. 1) is the most appropriate for the modeling of bagasse drying (Gilberd & Sheehan, 2013)(Vijayaraj et al., 2007)system COP and water outlets temperatures are investigated. Study shows that both the water mass flow rate and inlet temperature have significant effect on system performances. Test results show that the effect of evaporator water mass flow rate on the system performances and water outlet temperatures is more pronounced (COP increases 0.6 for 1 kg/min(Polanco, Kochergin, & Alvarez, 2013) The equilibrium moisture of bagasse can be calculated by the following equation-

$$MR = (M - M_e)/(M_o - M_e) = \exp(-kt^n) \quad \textbf{(Eq. 1)}$$

$$M_e = \frac{1800}{W} = \left(\frac{KH}{1 - KH} + \frac{K_1KH + 2K_1K_2K^2H^2}{1 + K_1KH + K_1K_2K^2H^2}\right) \quad \textbf{(Eq. 2)}$$

Table 1. Boiler information

Parameter	Value
Bagasse consumption rate	60 tph
Air inflow rate	190 tph
Flue gas exit temperature	141-155 °C
Amount of flue gas exiting	250 tph
Flue gas composition (% Vol)	CO_2 - 11.47; SO_2 - 0.00; O_2 - 3.72; H_2O - 25.36; N_2 - 58.75; Ar - 0.7

Table 2. Bagasse information

Parameter	Value
Bagasse moisture in	48 % (w/w)
Bagasse moisture out	30.0 % (w/w)
Bagasse temp (ambient)	30 C
Fresh bagasse density	150-200 kg/m³
Bagasse equivalent cylindrical diameter (Silva et al. 2012)	1.86 mm

Where, M = material moisture content (%), M_e = equilibrium moisture content in % dry basis, M_o = initial moisture content (%), k = drying rate coefficient (s^{-1}), n = empirical constant (dimensionless), t = required drying time (s), T = temperature (K), H = relative humidity (%). W, K, K_1, K_2 are all factors that can be solved by using the equations below-

$$W = -7.7 - 0.1982T + 22.305T^{0.5}$$

$$K = -2778.14 - 2042.09T + 5238.88T^{0.5}$$

$$K_1 = -70.42 - 13.68T + 180.22T^{0.5}$$

$$K_2 = -194.01 - 0.62T + 51.48T^{0.5}$$

The drying rate coefficient (k), can be determined by multiple regression analyses based upon the Page model constraints (Vijayaraj et al., 2007)system COP and water outlets temperatures are investigated. Study shows that both the water mass flow rate and inlet temperature have significant effect on system performances. Test results show that the effect of evaporator water mass flow rate on the system performances and water outlet temperatures is more pronounced (COP increases 0.6 for 1 kg/min(Polanco, Kochergin, & Alvarez, 2013)

$$k = 3.1094667E-03(H_d) - 3.1183596869E-03(T) - 3.947507753E-02(V) + 0.113762212(H_t) + 0.49123557038 \quad \textbf{(Eq. 3)}$$

Where, H_d = drying air humidity (g of wet air/kg of dry air), H_t = product thickness (mm). The empirical constant (n) is often calculated by the following equation-

$$n = -0.86990405 + 0.238750462 log(t) - 1.1754564904(k) \quad \textbf{(Eq. 4)}$$

However, the investigation has found that this constant can be let to equal n = 0.1485482 for the drying of bagasse (Vijayaraj et al., 2007) system COP and water outlets temperatures are investigated. Study shows that both the water mass flow rate and inlet temperature have significant effect on system performances. Test results show that the effect of evaporator water mass flow rate on the system performances and water outlet temperatures is more pronounced (COP increases 0.6 for 1 kg/min(Gilberd & Sheehan, 2013). Again, the dried bagasse is fluidized by drying gas (flue gas in this case) to ensure an even flow of bagasse and to reduce the chance of clumping of particles. The required terminal velocity (V_t) for the fluidization is selected by an empirical relation $V_t = 2.96 D_{hed}^{0.58}$ (Rasul, Rudolph, & Carsky, 1999), where D_{hed} is the equivalent diameter (mm). The flue gas compositions are supplied from the target company for the boiler (Table 6).

The humidity of the bagasse $H = (m_v/m_a)$ can be found using the molar volume of the flue gas at operating temperature (155C), where m_v = mass

Table 3. Feeder decision matrix

Feeder Specifications	Material Suitability	Feed Rate	Power Consumption	Maintenance and Reliability	Supporting Infrastructure	Total Score
Weighting	5	5	3	4	3	100
Screw feeder	5	5	3	4	3	84
Belt feeder	1	3	3	2	3	46
Rotary feeder	5	5	4	4	5	93

Table 4. Rotary feeder decision matrix

Company	Capacity	Physical Size	Power	Total
Rating	5	3	1	45
Young industries	2	5	5	30
Prater industries	2	5	5	30
Meyer	5	5	3	43

Table 6. Chemical composition of flue gas

	Wet Volume (%)	Molar Mass (g/mol)	Density (g/m³)
CO_2	11.47	44.01	1253.47
SO_2	0.00	64.06	1824.66
O_2	3.72	31.99	911.39
H_2O	25.36	18.02	513.11
Ar	0.7	39.95	1137.80
N_2	58.75	28.01	797.87

Table 5. Decision matrix for bagasse dryer concepts

Type	Real estate required	Headspace (height)	Structural work required	Installation/ Erection difficulty	Fan/Power required	Design complexity/ Maintenance	Capital costs	Total Score
Weighting	8	4	6	6	5	5	6	
Single-pass	Small (5)	Large (1)	Small (5)	Small (2)	Moderate (3)	Small (5)	Small (5)	156
Series	Moderate (3)	Small (4)	Moderate (3)	Moderate (4)	Small (5)	Moderate (3)	Moderate (3)	140
Parallel	Moderate (2)	Small (4)	Large (2)	Moderate (3)	Large (2)	Large (1)	Large (1)	83

of moisture present, m_a = total dry mass. Trial and error methods were conducted to determine the expected drying parameters at the low drying time. For an arbitrary volume of 10 m^3 bagasse, the calculation is made to obtain the mass of flue gases (Table 7) and drying parameters (Table 8). The drying time is within the expected range for a flash drying system.

According to the company, the estimated flue gas exiting from the boiler is m_{fg} = 227,672 kg/hr assuming ${}_{fg}$ = 1 kg/m^3 of gas flow. The bagasse flow rate is m_b = 60 tph assuming ${}_{b}$ = 150 kg/m^3 of bagasse flow. Calculating a total flow balance with the summation of the flue gas and bagasse flow, we can determine the desired diameter and length of the dryer (Table 9).

4.3 Parametric Study for Dryer

Due to the size restriction of a 6 6 25 m footprint for the bagasse drying system, the drying tube was optimized for both performance and design requirements emplaced by the company. The fluid mixture velocity influences the dryer length (Fig. 1(a)). As the dryer length should be kept to a minimum, it is advantageous to keep the fluid mixture velocity to a minimum; thus, the values calculated for the arbitrary volume of the bagasse (V = 6.742 m, and L = 4.61m) were kept fixed and used.

Table 7. Mass of flue gas composition

Compositions	Mass (g)
CO_2	1453.90
SO_2	0
O_2	342.75
H_2O	1316.21
Ar	80.544
N_2	4739.59

Table 8. Calculated drying parameters

Parameter	Value	Source
M	30%	Company
Mo	48%	Company
Me	5.67%	Eq. 2
T	423.15 K	Company
Dhed	1.86 mm	(Rasul et al., 1999)
Ht	1.86 mm	(Mujumdar, 2014)
H	19.89%	-
k	0.586	Eq. 3
V	6.742 m/s	Vt + 2.5m/s
MR	0.575	Eq. 1
t	0.684 s	Eq. 1

At fixed dryer length (L = 4.61m), it is necessary to reduce the dryer diameter (D) to limit the flow rate of flue gas into the dryer. The excess flue gas is directed to the exhaust stack as per the current operation. However, the optimum flow rate of the flue gas can be estimated at a particular dryer diameter using the figures presented in Fig. 1(b).

From this analysis, it has been determined that a flow rate of flue gas of 6 m^3/s, results in a dryer diameter of 1 m (Fig. 1(b)). This dimension allows for a minimal footprint while being comparable to the required inlet for the cyclone, thus reducing losses, and reducing the chance of bagasse becoming stuck and igniting during operation (Table 10).

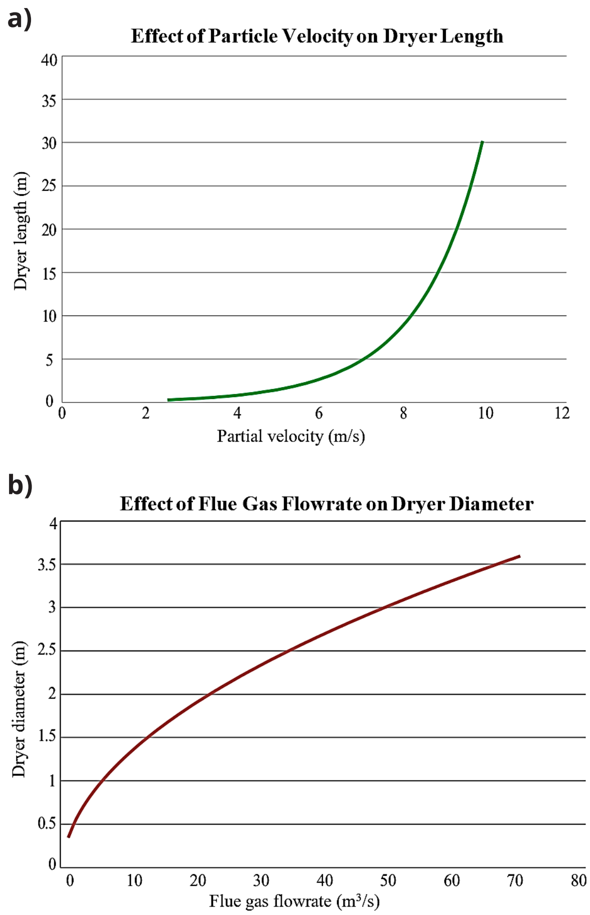

Fig. 1: (a) Effect of particle velocity on dryer length, (b) Effect of flue gas flowrate on dryer diameter

Table 9. Dryer dimension

Parameter	Mathematical relation	Value
Flue gas flow rate ($Q_{flue\ gas}$)	$m_{fg/}/g$	63.24 (m^3/s)
Bagasse flow rate ($Q_{bagasse}$)	$m_b/{}_b$	0.111 (m^3/s)
Total flow rate (Q_{total})	$Q_{bagasse} + Q_{flue\ gas}$	63.351 (m^3/s)
length of drying tube (L)	Vt	4.61 m
Diameter of dryer (D)	$[4Q_{total}/V]^{1/2}$	3.46 m

Heat Transfer Analysis of Drying Tube

Mass balance

Assuming the desired outlet bagasse moisture at 30% (as per the expected goal), an overall mass balance can be achieved as below-

$$_{fg.in}dry + _{fg.in}wet + _{bag.in}dry + _{bag.in}wet = _{fg.out}dry + _{fg.out}wet + _{bag.out}dry + _{bag.out}wet \quad \textbf{(Eq. 5)}$$

As the dry components of bagasse and flue gas are equal before and after the reaction, ignoring these parameters the modified mass balance equation is-

$$_{fg.in}wet + _{bag.in}wet = _{fg.out}wet + _{bag.out}wet \quad \textbf{(Eq. 6)}$$

This mass balance can be broken into its respective mass flowrates and moisture content as shown below-

$$M_{fg}\, m_{fg.in} + M_{bag}\, m_{bag.in} = M_{fg}\, m_{fg.out} + M_{bag}\, m_{bag.out} \quad \textbf{(Eq. 7)}$$

Calculated summary from the from the above equations, presented in Table 11 and Table 12.

4.4.2 Bagasse Exit Temperature

To calculate the temperature of bagasse particles at the exit of the drying tube, a lumped capacitance method is assumed with flue gas temperature of 150 C, bagasse properties are constant, bagasse particles are spherical and have no effect on neighboring particles. Using a free body diagram of the idealized case (Fig. 2) and using flue gas and bagasse properties (Table 13), the final bagasse temperature (T_f) can be determined using the following relation-

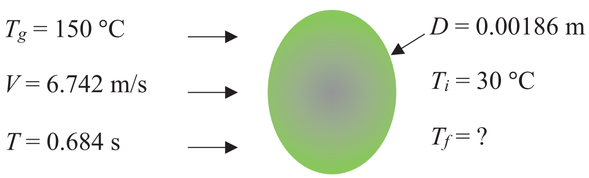

Fig. 2: Free body diagram of bagasse particle

$$T_f = T_g + \frac{1}{\exp\left(\frac{6th_{fg}}{d_s \rho C_p}\right)} \times (T_i - T_g) \quad \textbf{(Eq. 8)}$$

Using the empirical correlations for heat transfer coefficient available for gas-particle flows [6], we can determine the Reynolds number (*Re* = 387.16) and Nusselt number (*Nu* = 58.07) to obtain the value h_{fg} = 1164.52 W/m^{2}K as well as T_f = 67.96 C.

Heat Loss through Drying Tube

In order to determine the insulation, thickness the Fig. 3 and Fig. 4 was used and result summarized in Table 14.

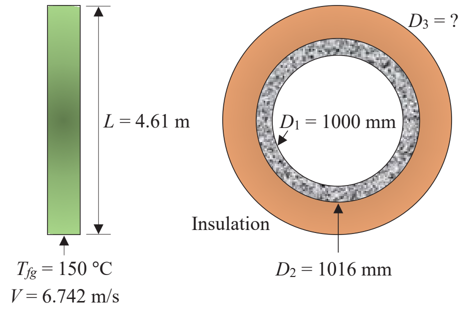

Fig. 3: Free body diagram of a drying tube. (Left) Side view, (right) internal view exaggerating layers.

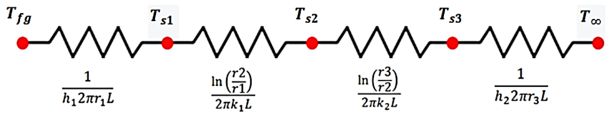

Fig. 4: Thermal circuit of bagasse drying tube

Table 14 summarizes the additional parameters used, and the correlations or equations used to find them. The heat transfer throughout the drying tube occurs via three mechanisms, (i) Convective (internal flow), (ii) Conductive (through drying tube, and insulation) and (iii) Convective (external flow) (Table 15).

An analysis is first conducted to find the outer surface temperature of the drying tube without insulation. The overall heat transfer rate is calculated by Eq. 9-10.

$$q_r = \frac{R_{fg} - T_\infty}{R_{tot}} \quad \textbf{(Eq. 9)}$$

$$R_{tot} = \frac{1}{h_1 2\pi r_1 L} + \frac{\ln\left(\frac{r_2}{r_1}\right)}{2\pi k_1 L} + \frac{1}{h_2 2\pi r_2 L} \quad \textbf{(Eq. 10)}$$

By establishing the overall heat transfer rate, we can conduct a simple nodal analysis, working from inside the drying tube to the outside. This analysis allows the determination of the inner (96.06 °C) and outer (95.96 °C) surface temperatures.

Knowing the outer temperature of the drying tube, we can now specify an appropriate insulative material. A500 Insulative paint (Product catalogue, Insulpaint Australia Pty Ltd, 2004) from Insulpaint Australia was chosen to

Table 10: Final design parameters

Parameter	Value
Bagasse feed rate	60 tph
Bagasse moisture in	48%
Bagasse moisture out	30%
Flue gas flow rate	6.0 m^3/s, (21,600 m^3/hr)
Flue gas temperature	150 °C
Fluid mixture velocity	6.742 m/s
Drying tube diameter	1 m

Table 11: Summary of mass balance values

	Flowrate (*M*) [kg/s]	Moisture (*in*) (%)	Moisture (*out*) (%)
Bagasse	16.65	48	30
Flue Gas	6.0	19.85	70

be applied to the outside of the drying tube. A parametric study to find an appropriate thickness of insulation was conducted (Fig. 5). Including insulation, R_{tot} becomes,

$$R_{tot} = \frac{1}{h_1 2\pi r_1 L} + \frac{ln\left(\frac{r_2}{r_1}\right)}{2\pi k_1 L} + \frac{ln\left(\frac{r_3}{r_2}\right)}{2\pi k_2 L} + \frac{1}{h_2 2\pi r_3 L} \quad \textbf{(Eq. 11)}$$

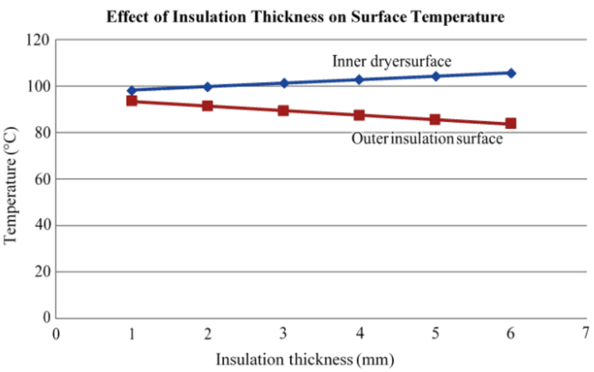

Fig. 5: Parametric study, investigating the effects of insulation thickness and surface temperature.

It is recommended that a paint coating of between 2-5 mm be applied. Assuming a coating of 4 mm, Table 16 summarizes the calculated surface temperatures for completeness.

4.4.4 Flue Gas Exit Temperature

To calculate the exit temperature of the flue gas, the overall energy balance has been considered as shown in Fig. 6. It should be noted that the "one bagasse particle" is a total representation of all the individual particles in the dryer. The overall balance is described below-

$$Q_{out} = q_{in} - (q_{bag} + q_{wall}) \quad \textbf{(Eq. 12)}$$

Table 12: Summary of flue gas (dry and wet) mass flowrates.

Parameter	Flowrate [kg/s]
Dry Flue Gas (*in*)	4.809
Wet Flue Gas (*in*)	1.191
Dry Flue Gas (*out*)	1.8
Wet Flue Gas (*out*)	4.2

Table 13: Flue gas and bagasse properties

Parameter	Value
***Flue gas* (@ 150 C)**	
Dynamic viscosity (ϑ)	32.39 10^{-6} m^2/s
Thermal conductivity (k)	0.0373 W/mK
Prandtl Number (Pr)	0.686
***Bagasse* (@ 30 C)**	
Density (ρ)	150 kg/m^3
Heat capacity (C_p)	0.7508 kJ/kgK

From Table 16 the overall heat transfer rate out of the dryer wall is 8034.93 W with a 4 mm insulative paint applied. Therefore the Eq. 12 can be solved for all other parameters.

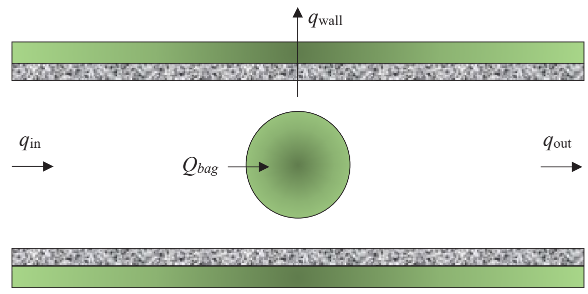

Fig. 6: Overall energy balance for the drying tube.

4.4.5 Heat Transfer into Bagasse

In works published by Mujumdar (Mujumdar, 2014), the heat transfer rate (per volume) between and gas and solid phase can be calculated via the following Eq. 13.

(W/m^3) **(Eq. 13)**

where, = solid volume fraction in the mixture, d_s = diameter of bagasse particle (m), h_{gs} = heat transfer coefficient (W/m^2K), T_g = temperature of the gas, and T_s = average temperature of the bagasse. The solid volume fraction is calculated as = $Q_b/(Q_b+Q_g)$ = 0.111/(0.111+6.0) = 0.01816. Using the Baeyens et al. (Maurice, Mezhericher, Levy, & Borde, 2015) correlation for the Nusselt's number, the heat transfer coefficient can be established and the heat transfer rate calculated (Table 17).

Table 14: Summary of known parameters/properties

Parameter/Properties	Value
Flue gas temperature (T_{fg})	150 C
Drying tube length (L)	4.62 m
Velocity flue gas (V)	6.742 m/s
Ambient air temperature ( )	27 C
Ambient air velocity	3.11 m/s [20]
Drying tube inner diameter (D_1)	1000 mm
Drying tube thickness	8 mm
Drying tube outer diameter (D_2)	1016 mm
Insulation thickness	?
Insulation outer diameter (D_3)	?
Inner drying tube surface (T_{s1})	?
Surface between dryer and insulation (T_{s2})	?
Outer insulation surface (T_{s3})	?
Flue Gas @ 150	
Dynamic viscosity	32.39 10^{-6} m^2/s
Thermal conductivity (k_f)	0.0373 W/mK
Prandtl Number (Pr_f)	0.686
Air @ 27 C	
Dynamic viscosity ($_a$)	15.89 10^{-6} m^2/s
Thermal conductivity (k_a)	0.0263 W/mK
Prandtl Number (Pr_a)	0.707

Table 15: Calculated parameters for heat transfer analysis

Parameter	Value	Equation/Correlation
Internal flow		
Reynolds number (Re)	208,150.60	$Re = V_{fg}D_1/v_f$
Friction factor (f) (as turbulent flow)	0.01549	Petukhov's correlation
Nusselt number (Nu)	314.156	Gnielinski correlation
Heat transfer coefficient (h_1)	11.718 W/m^{2}K	$h_1 = (Nu)(k_f)/D_1$
External flow		
Reynolds number (Re)	195,790.50	$Re = V_aD_3/v_a$
Nusselt number (Nu)	343.04	Churchill and Bernstein correlation
Heat transfer coefficient (h_2)	9.022 W/m^{2}K	$h_2 = (Nu)(k_a)/D_1$
Conduction (Dryer)		
Thermal conductivity of wrought carbon steel (k_1)	58.82 W/mK	[21]
Conduction (Insulation)		
Thermal conductivity of Insulpaint (A500) (k_2)	0.142 W/mK	[22]

Thus, by substituting the known values into Eq. 13, we can solve the heat transfer rate (per volume) into a singular bagasse particle as q_{gs} = q_{bag} = 6,892,047.57 W/m^3. Knowing the volume of one particle the heat transfer rate into one particle is q_{bag} = 0.02322 W, the total heat transfer rate can be found as $q_{bag,\ tot}$ = 765541 W.

Table 16: Summary of surface temperatures with 4 mm insulation.

Parameter	Value
Insulation thickness	4 mm
Insulation outer diameter (D_3)	1024 mm
Overall heat transfer rate (q_r)	8034.93 (W)
Inner drying tube surface (T_{s1})	102.757
Surface between dryer and insulation (T_{s2})	102.682
Outer insulation surface (T_{s3})	87.394

4.4.6 Heat Transfer Rate In and Out

To calculate the energy at the inlet and outlet of the drying tube, an analysis of the flue gas enthalpy was conducted, assuming constant pressure throughout. Expressions for the enthalpy at the inlet and outlet are presented below (Eq. 14-15). Table 18 summarizes the parameters used to solve the enthalpy analysis.

$$q_{in} = H_{fg,in} = M_{fg\ dry\ in}\, C_p T_{fg\ in} + M_{fg\ wet\ in}\,(h_v + C_{ps} T_{fg\ in}) \quad \textbf{(Eq. 14)}$$

$$q_{out} = H_{fg,out} = M_{fg\ dry\ out}\, C_p T_{fg\ out} + M_{fg\ wet\ out}\,(h_v + C_{ps} T_{fg\ out}) \quad \textbf{(Eq. 15)}$$

Table 18: Summary of parameters involved in the enthalpy energy balance (Note: Constant thermal properties are assumed throughout)

Thus, Eq. 14 and Eq. 15 gives q_{in} = 5593055 W and q_{out} = 8876280 + 10224.108$T_{fg\,out}$ respectively. By subbing all components into Eq. 15, we can solve the outlet temperature $T_{fg\ out}$ = 396.8 K = 123.8 C. Table 19 below summarizes the parameters determined via the heat and mass analysis as described above.

4.5 Cyclone separator

In the case of separating the dried bagasse from the moisture-rich flue gas exiting the dryer the most common form of the dry scrubber is a cyclone separator (Strumiłło, L. Jones, & Żyłła, 2014)(Moor, 2007)(Bashir, 2015)(Pynadathu, Thomas, & Arjun, 2014). The most common type of dryer is shown in Fig. 7. Over the last 50 years, the design and optimization of cyclones have been extensively investigated by researchers such as Stairmand, Swift 1, Lapple, Swift 2 and Peterson/Whitby (Leith, 1990). Each design determines the various component lengths and diameters as a function of the body diameter (D) as outlined below in ref (Leith, 1990).

From this review of the literature and consultation with the company (required throughput rate of 60 tph), a high throughput cyclone is required. The scheme chosen is the Swift scheme (Leith, 1990) which is a function of the input flow rate, inlet velocity and combined density (Table 20).

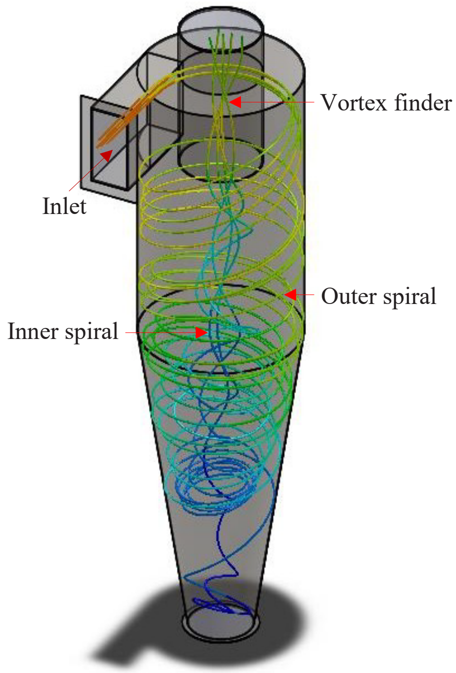

Fig. 7: Cyclone vortices

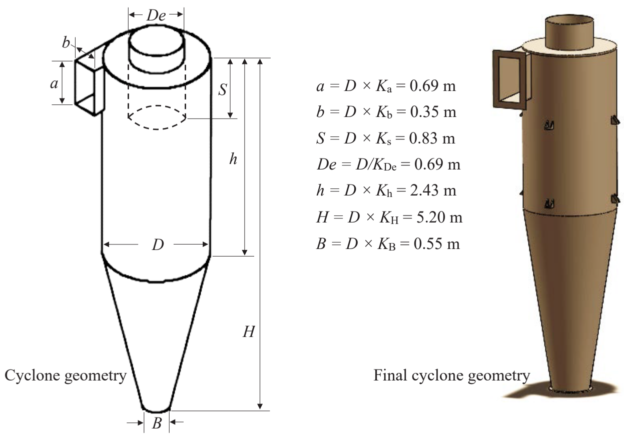

Fig. 8: Cycle parameters as standard in reference (Utikar et al., 2010)

Table 17: Summary of parameters for calculating bagasse heat transfer rate.

Parameter	Value
Diameter of bagasse (d_s)	0.00186 m
Temperature of flue gas (T_g)	150
Average temperature of bagasse (T_s)	49
Dynamic viscosity	32.39 10^{-6} m^2/s
Velocity of flue gas (V)	6.742 m/s
Thermal conductivity flue gas (k)	0.0373 W/mK
Reynolds number (Re)	387.16
Nusselt's number (Nu)	58.07
Heat transfer coefficient (h_{fg})	1164.6 W/m^2K

Table 18: Summary of parameters involved in the enthalpy energy balance (**Note:** Constant thermal properties are assumed throughout)

Parameter	Inlet	Outlet
Mass flowrate flue gas (*dry*)	4.809 kg/s	1.8 kg/s
Mass flowrate flue gas (*wet*)	1.191 kg/s	4.2 kg/s
Temperature flue gas	423 K	?
Specific heat (C_p) air		1.01722 kJ/kgK
Specific heat water vapor (C_{ps})		1.99836 kJ/kgK
Water heat of vaporization (h_v)		2113.4 kJ/kg

Table 19: Summary of heat and mass analysis.

Parameter	Value
Moisture content bagasse (exit)	30%
Moisture content flue gas (exit)	4.2 kg/s (70%)
Temperature bagasse (exit)	67.96 C
Temperature flue gas (exit)	123.8 C
Insulation thickness	2-5 mm

The main diameter is calculated and found to be $D = 1.39$ m ($D = 0.0166709(\frac{Q}{VK_b})^{0.5}$) according to the ref. (Leith, 1990). In reference to Fig. 8, the following equations describe the functional relationships between the major diameter and the other functional variables (Bashir, 2015)(Leith, 1990).

The pressure drops = 13.38 cm of water () across the cyclone is a function of the velocity heads at the inlet and outlet $N_H = 3.804$ ($N_H = (K_{VH})(ab)/De^2$), the density of the gas (kg/m^3), and the velocity of the inlet (v_i m/s). Using the Shepard and Lapple empirical relationship for velocity heads at the inlet and outlet of the cyclone, the empirical constant has a value $K_{VH} = 16$ for tangential inlets and $K_{VH} = 7.5$ for cyclones with an inlet vane [10].

Specification of Fan

A forced draught fan is installed upstream of the drying tube to ensure the desired flue gas flowrate is achieved. To ensure the correct specification of the fan, the losses in the system must be considered. This can be achieved by applying a control volume (Fig. 9) and solving Bernoulli's equation (Eq. 16).

$$h_{fan} = \frac{P_2 - P_1}{\rho g} + \frac{V_2^2 - V_1^2}{2g} + (z_2 - z_1) + h_{L,1-2} \qquad \textbf{(Eq. 16)}$$

where, P - absolute pressure (Pa), V - velocity (m/s), z - elevation (m), $h_{L,1\text{-}2}$ - head loss (m). The $h_{L,1\text{-}2}$ can also be described as $h_{L,1\text{-}2} = h_{dryer} + h_{cyclone}$. Table 22 below contains the parameters, equations, and assumptions made to solve for the required fan head.

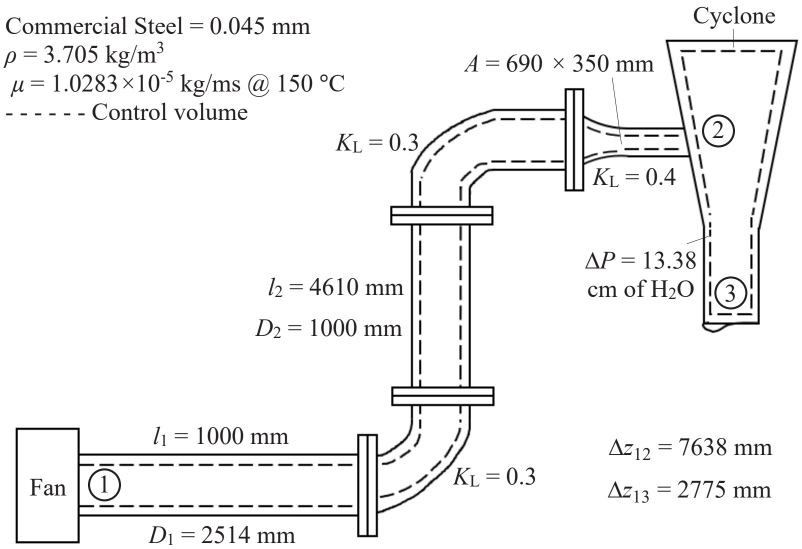

Fig. 9: Control volume of the drying system

The head loss through the dryer can be calculated via Eq. 17

$$h_{dryer} = \left(f\frac{L}{D} + K_{L,minor}\right)\frac{V^2}{2g} \qquad \textbf{(Eq. 17)}$$

while the head loss due to the pressure drop in the cyclone can be found via $h_{\text{dryer}} = \Delta P/\rho g$. With the given information, Eq. 16 can be solved (Table 23).

To be able to source parts and spares nationally a fan will be selected from Aerotech (Company catalogue, Aerotech Fans Pty. Ltd.). It has been determined that a centrifugal pump is most suited for the bagasse drying system. From these options, it is apparent that the MAVX405 (Table 24) (Company catalogue, Aerotech Fans Pty. Ltd.) is the only option that satisfies our criteria. It has the required flow rate, while also having a large enough static pressure head for our requirements.

Drying Tube Selection

After consultation with the company about the importance of design aspects and design requirements, a weighted decision matrix (Ouye, Facility Technics Facility Management Consulting) was devised (Table 25) and determined that the single-pass circular drying tube is the most appropriate and accepted by company engineers.

Proposed Structure

After determining all dryer design parameters and parts specifications, this paper proposes an improved design for the bagasse drying system for the boiler of the cogeneration plant (Fig. 10). A scale model of the overall structure of the proposed design has drawn (Fig. 10), which included all the parts (feeders, fan, drying tube, and cyclone). All parts of the proposed design (Fig. 10) are supported by a structure that fits within the specified area of the mill without hindering

Table 20: Swift cyclone design input parameters and values

Parameter	Value
Input flow rate (m^3/h)	21,600
Inlet velocity (m/s)	25
Gas density (kg/m^3)	1.0

Table 21: Constant values for diameter and length determination

Value	Stairmand	Swift	Lapple	Swift	Peterson/Whitby
K_D	0.1	0.0924	0.125	0.125	0.121264
K_a	0.5	0.44	0.5	0.5	0.583
K_b	0.2	0.21	0.25	0.25	0.208
K_s	0.5	0.5	0.625	0.6	0.583
K_{De}	2	2.5	2	2	2
K_h	1.5	1.4	2	1.75	1.333
K_H	4	3.9	4	3.75	3.17
K_B	0.375	0.4	0.25	0.4	0.5

Table 22: Parameters used for specification of fan

Parameter	Value	Comments
Dryer/Feeder		
Length	7124 mm	Elbow-length is excluded
Diameter	1000 mm	
Flowrate	6 m3/s	
Roughness ()	0.045 mm	Commercial Steel
Standard flanged elbow minor loss factor (×2)	KL = 0.3	
Reducer minor loss factor	KL = 0.4	
Friction factor (f)	0.01145763	Using Swamee-Jain equation (Towler & Amherst, 2012)
Cyclone		
Inlet dimensions	690 × 350 mm	
Inlet velocity	24.85 m/s	
Length	4865 mm	
Pressure drops through the cyclone	13.38 cm of H2O	
Fluid Properties & Other		
Mixture density	3.705 kg/m3	
Viscosity	1.0283×10-5	Assume fluid viscosity of air at 150 °C
Reynolds number	2,752,515.32	
Inlet pressure	101,325 Pa	Atmospheric, as per J. Gilberd (Gilberd & Sheehan, 2013)
Outlet pressure	101,325 Pa	
Elevation	(in Fig. 9)	

Table 23: Calculated Fan Head

Parameter	Value
$h_{L,1\text{-}2}$	14.618 m
$h_{L,cyclone}$	36.04 m
h_{fan}	86.782 m
Static pressure	3154.18 Pa
Flow rate required	21,600 m^3/hr

Table 24: MAVX405 properties compared to requirements

Parameter	Required	Fan Capabilities
Static Pressure	3.154 kPa	3.5 kPa
Volume flow rate	6.0 m^3/s	0-20 m^3/s
Power requirement	-	130 kW
Efficiency	-	82.2 %

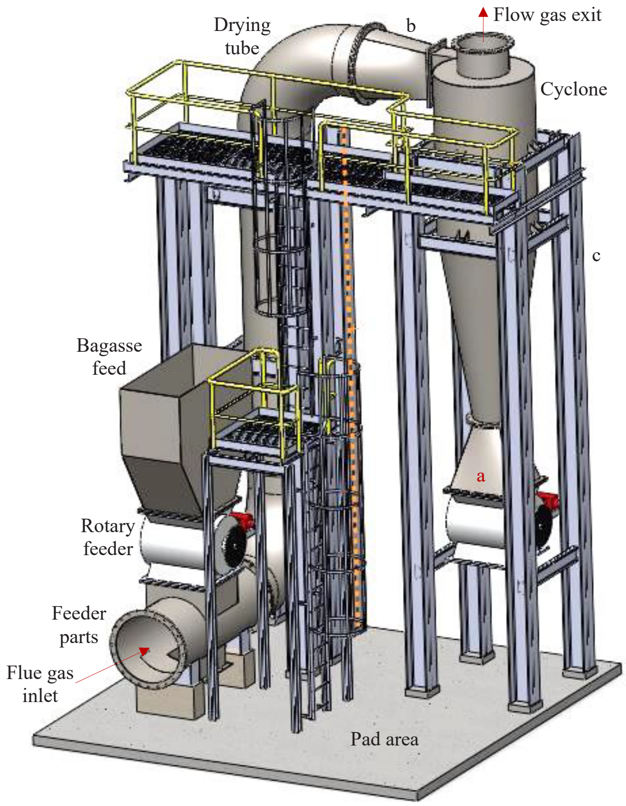

Figure 10. Overall proposed design. a: Bagasse exit; b: Feed point for water suppression system; c: Structure

any accessibility problem. The proposed design can be constructed in-place to dry the bagasse. Since all the parts and specifications for this design are derived for industrial scale, it will be easy to modify the proposed design with necessary bagasse and boiler information for any kind of industrial bagasse drying system.

Conclusion

This work has analyzed the step by step boiler and bagasse information for a case-study based problem to determine all dryer design parameters and parts specifications for an industrial scale bagasse drying system. The proposed design will be capable of drying bagasse and reducing moisture content from 48% to 30% for the boiler of the cogeneration plant. The selected feeder for

Table 25: Decision matrix for bagasse dryer tube selection

Score 1 - Poor 5 - Good	Real Estate Required	Head Space (Height)	Structural Work Required	Installation/ Erection Difficulty	Fan/ Power Required	Design Complexity/ Maintenance	Capital Costs	Total Score
Weighting	×8	×4	×6	×6	×5	×5	×6	
Single Pass	Small (5)	Large (1)	Small (5)	Small (2)	Moderate (3)	Small (5)	Small (5)	156
Series	Moderate (3)	Small (4)	Moderate (3)	Moderate (4)	Small (5)	Moderate (3)	Moderate (3)	140
Parallel	Moderate (2)	Small (4)	Large (2)	Moderate (3)	Large (2)	Large (1)	Large (1)	83

the proposed design is 36 36 inch, 20 RPM, Meyer rotary feeder for a drying tube of length 4.61 m having 3.46 m diameter. However, with a trial-based optimization for 60 tph of bagasse flow and 150 C of flue gas temperature, the diameter can be reduced to 1 m for certain estimated dying. In the proposed design the drying tube will have insulation of 4 mm thickness and will be painted with a heat protected coating. The separation of the flue gas and bagasse will occur in a flash cyclone separator. The design is planned to be operated by a centrifugal forced draught pump and the selected drying tubes are single-pass circular type. On the basis of this design analysis and specifications, an efficient industrial scale bagasse drying system can be placed in any sugar mill cogeneration plant to achieve a moisture reduction. However, this work reserves the following points for future research: Structural design analysis of all components, Estimated cost for the overall setup, Installation and run

References

Abdalla, A. M.; Hassan, T. H.; Mansour, M. E. 2018. Performance of wet and dry bagasse combustion in assalaya sugar factory - Sudan. *Innovative Energy & Research*, 7(1), 179. https://doi.org/10.4172/2576-1463.1000179

AS/NZS ISO 31000:2009. (2009). *Risk management – principles and guidelines superseding, Australia Standard*. https://infostore.saiglobal.com/preview/293451727151.pdf?sku=119718_SAIG_AS_AS_274522

Bashir, K. 2015. Design and fabrication of cyclone separator. BS thesis, Department of Chemical Engineering, University of Gujarat. India. 35p. http://dx.doi.org/10.13140/RG.2.2.20727.83368

Borde, I.; Levy, A. 2006. Chapter 16: *Pneumatic and flash drying*. In: Ed. Mujumdar, A. S. *Handbook of Industrial Drying*. (3rd ed.). Taylor & Francis Group. CRC Press. London. 1312 p.

Company catalogue on Rotary Airlock Feeders 2014. Smoot Inc. https://www.magnumsystems.com/wp-content/uploads/2017/09/MAG-Airlock-Br-7.pdf

Gilberd, J.; Sheehan, M. 2013. Modelling the effects of bagasse pre-drying in sugar mill boiler systems. *Proceedings of the 35th Conference of the Australian Society of Sugar Cane Technologists*, Townsville, QLD, Australia.

Leith, D. 1990. Cyclone performance and design. 20th Quarterly Report, US Department of Energy, DOE/PC/79922--T5, DE91 002492. https://www.osti.gov/servlets/purl/6273743

Maurice, U.; Mezhericher, M.; Levy, A.; Borde, I. 2015. Drying of droplets containing insoluble nanoscale particles: second drying stage. *Drying Technology*, 33(15–16), 1837–1848. https://doi.org/10.1080/07373937.2015.1039540

Moor, B. 2007. Flue gas scrubbing equipment for bagasse fired boilers. *Proceedings of International Society of Sugar Cane Technologist*s, 26, 1273–1283.

Mujumdar, A. S. 2014. *Handbook of industrial drying* (4th ed.). Taylor & Francis. CRC Press. London. 1348 p. https://doi.org/10.1201/b17208

Ouye, J. (n.d.). Weighted criteria matrix. Facility Technics Facility Management Consulting, 505 17th Street, Suite 300, Oakland, CA 94612. https://cpb-us-e1.wpmucdn.com/blogs.cornell.edu/dist/a/3723/files/2013/09/Weighted-Criteria-Matrix-1fxfcuw.pdf

Polanco, L. S.; Kochergin, V.; Alvarez, J. F. 2013. Fluidized bed superheated steam dryer for bagasse: effects of particle size distribution. *Journal of Sustainable Bioenergy Systems*, 3(4), 265–271. https://doi.org/10.4236/jsbs.2013.34036

Product catalogue: A500 INSULPAINT. 2004. Energy saving reflective/waterproofing coating, Insulpaint Australia Pty Ltd. https://www.insulpaint.com.au/downloads/A500_Insulpaint_data_sheet.pdf

Product catalogue (n.d.). Centrifugal Fans, Non-Overloading, Backward Inclined, Aerotech Fans Pty. Ltd., ISO 1940. https://www.aerotechfans.com.au/wp-content/uploads/2019/01/aerotech_download-07-product-catalogue-50-69.pdf

Pynadathu, N.; Thomas, P.; Arjun, P. 2014. *Engineering design & specifications of cyclone separator*. MTech (Energy & Environmental Engineering) SMBS, VIT-University, India. https://www.scribd.com/document/462569108/FINALREPORT

Raj, L. P.; Stalin, B. 2016. Optimized design of a bagasse dryer system for sugar industry. *Bonfring International Journal of Industrial Engineering and Management Science*, 6(4), 115–119. https://doi.org/10.9756/BIJIEMS.7536

Rasul, M. G.; Rudolph, V.; Carsky, M. 1999. Physical properties of bagasse. *Fuel*, 78(8), 905–910. https://doi.org/10.1016/S0016-2361(99)00011-3

Ravichandran, D.; Kavinkumar, V.; Kumar, K. M.; Prasanth, M.; Ramkumar, T. 2017. Design and analysis of bagasse dryer for boiler. *International Journal of Intellectual Advancements and Research in Engineering Computations*, 5(2), 1688-1691. https://ijiarec.com/ijiarec

Shanmukharadhya, K. S.; Sudhakar, K. G. 2007. Effect of fuel moisture on combustion in a bagasse fired furnace. *Journal of Energy Resources Technology, Transactions of the ASME*, 129(3), 248–253. https://doi.org/10.1115/1.2748816

Shrivastav, S.; Hussain, I. 2013. Design of bagasse dryer to recover energy of water tube boiler in a sugar factory. *International Journal of Science and Research*, 2(8), 356–358. https://www.ijsr.net/archive/v2i8/MDIwMTMyMDc=.pdf

Silva, A. J. P.; Lahr, F. A. R.; Christoforo, A. L.; Panzera, T. H. 2012. Properties of sugar cane bagasse to use in OSB. *International Journal of Materials Engineering*, 2(4), 50–56. https://doi.org/10.5923/j.ijme.20120204.04

Silva, L. D. da; Schlindwein, M. M.; Vasconcelos, P. S.; Corrêa, A. S. 2017. Electricity cogeneration from sugarcane Bagasse in Mato Grosso Do Sul, Brazil. *International Journal Advances in Social Science and Humanities*, 5(3), 11–26.

Sosa-Arnao, J. H.; Nebra, S. A. 2009. Bagasse dryer role in the energy recovery of water tube boilers. *Drying Technology*, 27(4), 587–594. https://doi.org/10.1080/07373930802716326

Strumiłło, C., L.; Jones, P.; Żyłła, R. 2014. Chapter 46: *Energy aspects in drying*. In Arun S. Mujumdar (Ed.), *Handbook of Industrial Drying* (4th ed.) Taylor & Francis.

To, L. S., Seebaluck, V.; Leach, M. 2018. Future energy transitions for bagasse cogeneration: Lessons from multi-level and policy innovations in Mauritius. *Energy Research and Social Science*, 35, 68–77. https://doi.org/10.1016/j.erss.2017.10.051

Towler, B.; Amherst, U. 2012 *Swamee-Jain friction factor*. https://en.smath.com/wiki/GetFile.aspx?File=Examples/Swamee-Jain%20friction%20factor%20for%20pipe%20flow%20121231.pdf

Utikar, R.; Darmawan, N.; Tade, M.; Li, Q.; Evans, G.; Glenny, M.; Pareek, V. 2010. *Hydrodynamic simulation of cyclone separators*. In *IComputational Fluid Dynamics*, Hyoung Woo Oh (Ed.), InTech, http://www.intechopen.com/books/computational-fluid- dynamics/hydrodynamic-simulation-of-cyclone-separators

Vijayaraj, B.; Saravanan, R.; Renganarayanan, S. 2007. Studies on thin layer drying of bagasse. *International Journal of Energy Research*, 31(4), 422–437. https://doi.org/10.1002/er.1237

Yasseri, S. 2013. *The ALARP argument*. Safe Sight Technology, UK. https://www.researchgate.net/publication/274677545_The_ALARP_Argument